Available online at www.sciencedirect.com
SCIENCE DIRECT
Sensors and Actuators A 130–131 (2006) 54–61
SENSORS AND ACTUATORS A PHYSICAL
www.elsevier.com/locate/sna

Three-dimensional nanosprings for electromechanical sensors

D.J. Bell [a,*], Y. Sun [b], L. Zhang [c], L.X. Dong [a], B.J. Nelson [a], D. Grützmacher [c]

[a] *Swiss Federal Institute of Technology (ETH) Zürich, Switzerland*
[b] *University of Toronto, Canada*
[c] *Paul Scherrer Institute, Villigen, Switzerland*

Received 2 June 2005; received in revised form 20 October 2005; accepted 30 October 2005
Available online 19 December 2005

Abstract

This paper presents the use of a novel fabrication technique to produce three-dimensional (3D) nanostructures with nanoscale features that can be used for electromechanical sensors. The process uses conventional microfabrication techniques to create a planar pattern in a SiGe/Si bilayer that then self-assembles into 3D structures during a wet etch release. An additional metal layer can be integrated for higher conductivity. Results from the fabrication of the structures are demonstrated. Nanomanipulation inside a scanning electron microscope (SEM) was conducted to probe the structures for mechanical and electrical characterization. The experimental characterization results were validated by finite element simulation.

Keywords: Nanospring; Nanocoil; Electromechanical sensors; Nanomanipulation; Nanofabrication; Microfabrication; Self-assembly

1. Introduction

Many three-dimensional (3D) helical structures with micro- and nano-features have been synthesized from different materials. Typical examples include carbon micro-coils based on amorphous carbon [1], carbon nanocoils based on carbon nanotubes [2], and zinc oxide nanobelts [3]. Because of their interesting morphology, as well as mechanical [4], electrical [5], and electromagnetic properties, potential applications of these nanostructures include micro and nanoelectromechanical systems (MEMS and NEMS) such as springs, magnetic field detectors, chemical or biological sensors, electromagnets, inductors, actuators, and high-performance electromagnetic wave absorbers.

A new method of creating structures with nanometer-scale dimensions has recently been presented [6] and can be fabricated in a controllable way [7]. The structures are created through a top-down fabrication process in which a strained nanometer thick heteroepitaxial bilayer curls up to form 3D structures with nanoscale features. Helical geometries and tubes with diameters between 10 nm and 10 μm have been achieved. Functional electrical or electromechanical nanostructures have not been demonstrated although a range of devices can be developed by varying the electrical properties of the bilayer structure during initial deposition and by depositing a third layer on top [8]. While efforts using this novel fabrication technique to create nanoelectromagnets have been described [9], its use for new types of electromechanical sensors is presented here. For this purpose, the flexible nanostructures serve as a mechanism to transduce force to displacement. Deformations can be detected either visually or by the piezoresistance change of the structure that directly indicates applied forces. Both sensing mechanisms have been demonstrated previously with structures on the micrometer scale. For example, the deformation of polysilicon beams has been detected visually to measure forces generated by living cells [10], and piezoresistive microcantilevers have been used to characterize low-force electrical contacts [11]. Piezoresistive nanosensors based on the nanostructures presented in this paper promise great performance, as it is known that the piezoresistance of silicon increases with a decrease in cross-sectional area [12].

Characterization and fabrication of nanosensors have proven challenging problems. Previously, the mechanical response of carbon nanosprings was characterized with an atomic force microscope (AFM) [13]. In this paper, nanomanipulation [14] inside an SEM is applied for characterizing electromechanical properties of the nanostructures.

* Corresponding author. Tel.: +41 16323581.
E-mail address: dbell@ethz.ch (D.J. Bell).

0924-4247/$ – see front matter © 2005 Elsevier B.V. All rights reserved.
doi:10.1016/j.sna.2005.10.057

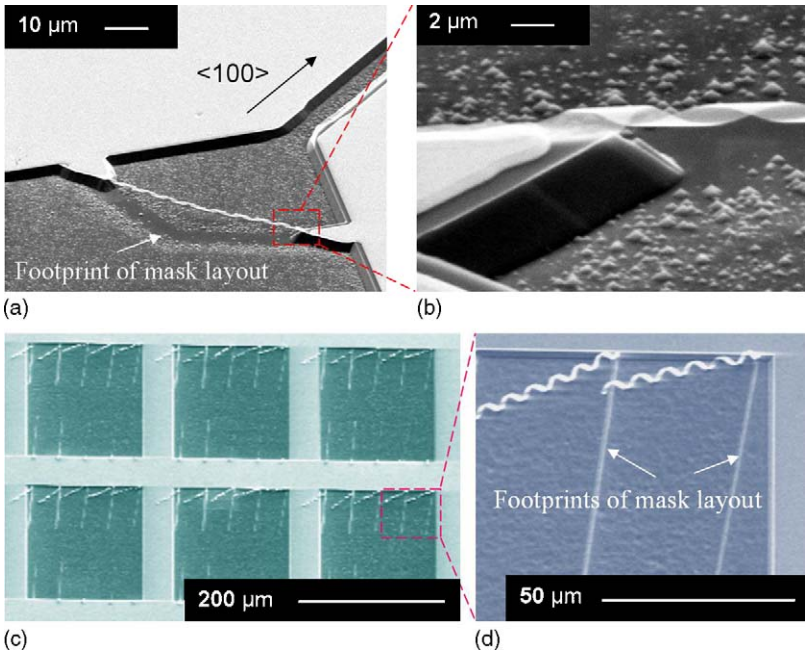

Fig. 1. SEM images of helical structure. (a and b) Fixed on both sides with length = 50 μm, diameter = 1.2 μm, bilayer thickness = 20 nm, and additional metal contacts for electrical devices. (c and d) Fixed on one side with length = 40 μm, diameter = 3.4 μm, bilayer thickness = 20 nm with additional 21 nm Cr layer in the nanospring.

2. Fabrication

Fig. 1 shows SEM images of typical helical nanostructures. In Fig. 1a and b, the nanospring is fixed on both sides after fabrication. The helical structure self-assembled between the two electrodes. The two halves of the nanospring have opposite winding directions. In Fig. 1c and d, nanosprings are fixed on one side only after fabrication. Fig. 2 illustrates the fabrication process for both types of nanosprings. One-side-polished 4 in. N-type float zone ⟨1 0 0⟩ Si wafers with high resistivity (10 kΩ cm) were used in order to minimize current leakage through the substrate (Fig. 2a). The heteroepitaxial SiGe/Si bilayers were grown by ultrahigh vacuum chemical vapor deposition (UHV/CVD) at 550 °C. The thickness of the epi-grown layers was always smaller than the critical thickness to maintain elastic strain in the SiGe film [15] (Fig. 2b and c). For selectively etching the low-doped ($\sim 10^{14}$ cm^{-3}) Si substrate under the SiGe/Si heterostrucutres, the SiGe/Si bilayers were heavily boron doped (p+) to a level of 2×10^{20} cm^{-3}. The initial pattern can be created through photolithography or E-beam lithography depending on the required feature size. S1813 was used as a resist for photolithography and PMMA for E-beam lithography (Fig. 2d). After the development of the resist (Fig. 2e), RIE with a mixture of SF_6, CHF_3 and O_2 gases was used to transfer the pattern to the SiGe/Si bilayers at an etch rate of approximately 1 nm/s (Fig. 2f). For the self-assembly of the nanostructures, samples were etched in 3.7% NH_4OH aqueous solution (Fig. 2h). The main advantages of NH_4OH–H_2O are that it does not incorporate alkaline ions which can contaminate CMOS integrated circuits, it is non-toxic, and it provides a higher selectivity to p+ SiGe/Si bilayers (8000:1) than KOH [16]. During wet etch, the patterned bilayer curled up along the ⟨1 0 0⟩ direction releasing

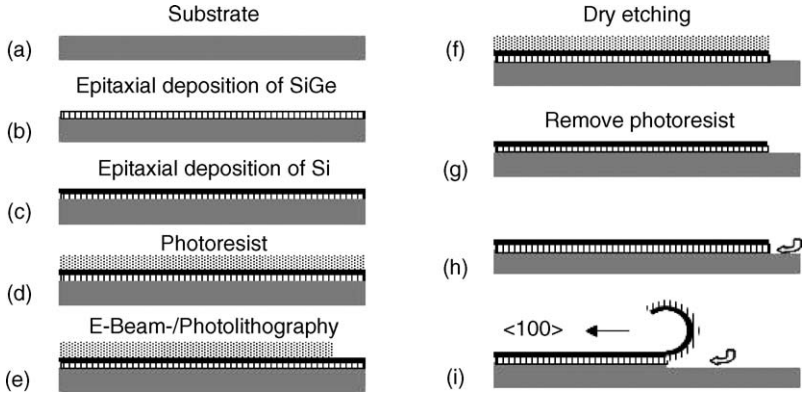

Fig. 2. Basic process sequence: initial planar bilayer, patterned through conventional microfabrication techniques assembles itself into 3D nanostructures during wet etch release.

the internal strain and forming 3D structures (Fig. 2i). Then the samples were rinsed in deionized water and subsequently in isopropyl alcohol. Finally, they were dried with a supercritical CO_2 dryer.

An additional Cr layer was integrated on top of the bilayer in some of the nanostructures, which curled up together with the bilayer. The Cr layer was deposited by thermal evaporation. The pattern was transferred into the Cr layer by Cl_2 and CO_2 plasma etching before dry etching the bilayer and subsequent NH_4OH–H_2O wet etch release.

3. Characterization experiments

For the characterization experiments, a nanomanipulator (Kleindiek, MM3A), an AFM cantilever (Nanoprobe, NP-S, stiffness 0.06 N/m), and a Tungsten wire (Picoprobe, T-4-10) were installed inside an SEM (Zeiss, DSM 962). The experimental procedure is illustrated in Fig. 3. A metal probe (Picoprobe, T-4-10-1 mm) with a tip radius of 100 nm, mounted on the nanomanipulator was first dipped into a conductive sticky tape (Ted Pella, Silver Conductive Sheet) in order to coat the probe with conductive glue (Fig. 3a and b). Then, the probe was used to break and pick up a nanospring (Fig. 3c). For the mechanical characterization, the AFM tip was dipped into the glue attached on the probe in order for the nanospring to be attached to the AFM cantilever. Finally, a tensile force was applied to the nanospring by moving the probe away from the AFM cantilever in the axial direction of the nanospring (Fig. 4). Five continuous frames of images were taken to detect the deflection of the cantilever and the relative displacement of the probe from the AFM cantilever. When the tensile force was increased further after the fifth measurement point, the attachment between the nanospring and the AFM cantilever broke (Fig. 4c).

A similar manipulation procedure was used for electrical property characterization. Instead of connecting the nanospring on one side to the AFM cantilever, it was connected to the Tungsten wire (Picoprobe, T-4-10), as illustrated in Fig. 4a. With this configuration the electromechanical response of a nanospring can be characterized (Fig. 5b and c).

4. Results and discussion

The SEM images were analyzed to extract the AFM tip displacement and the nanospring deformation, i.e. the relative displacement of the probe from the AFM tip. From this displacement data and the known stiffness of the AFM cantilever, the tensile force acting on the nanospring versus the nanospring deformation was plotted. The deformation of the nanospring

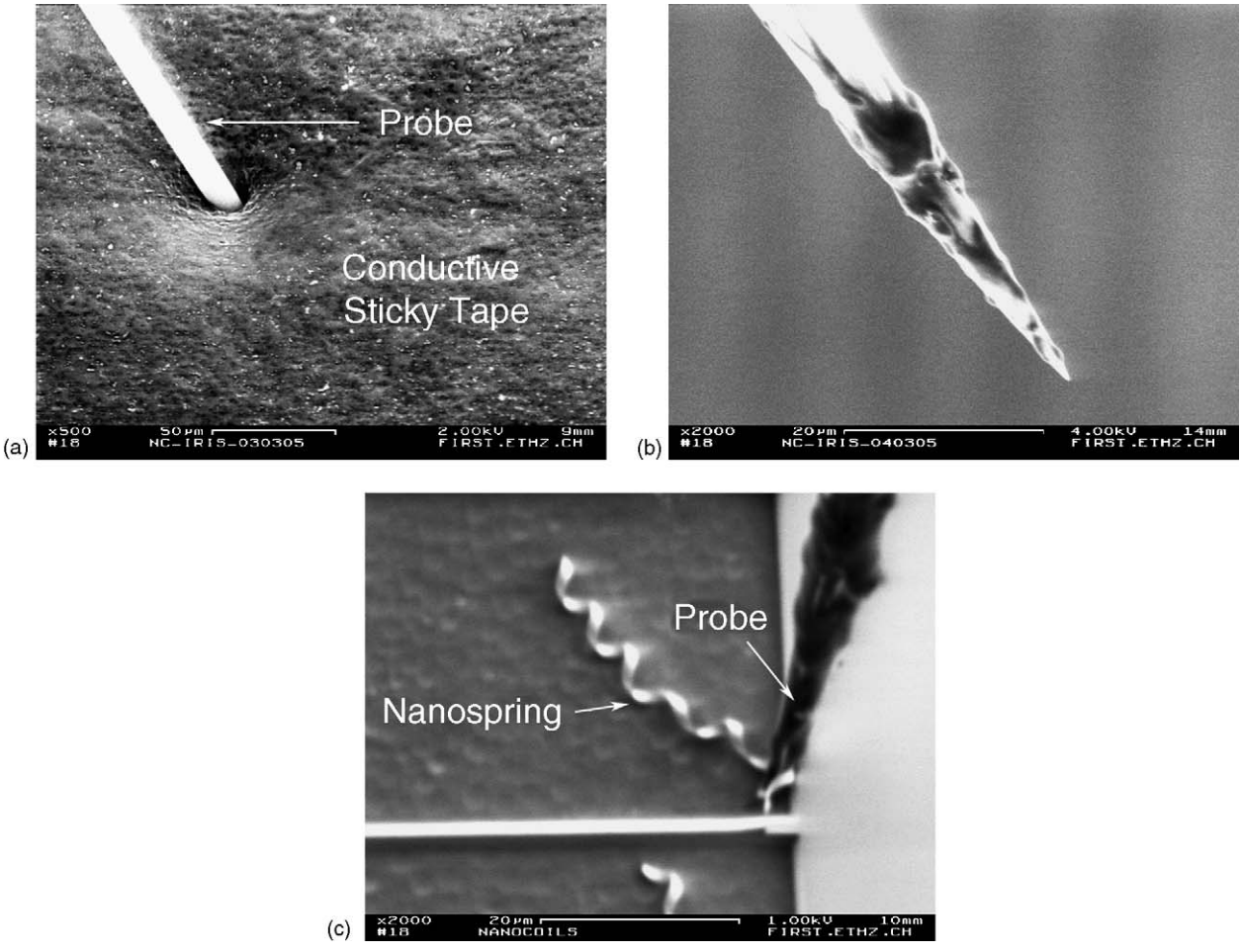

Fig. 3. "Sticky probe": (a) dip in SEM-tape, (b) probe tip and (c) picking up nanospring.

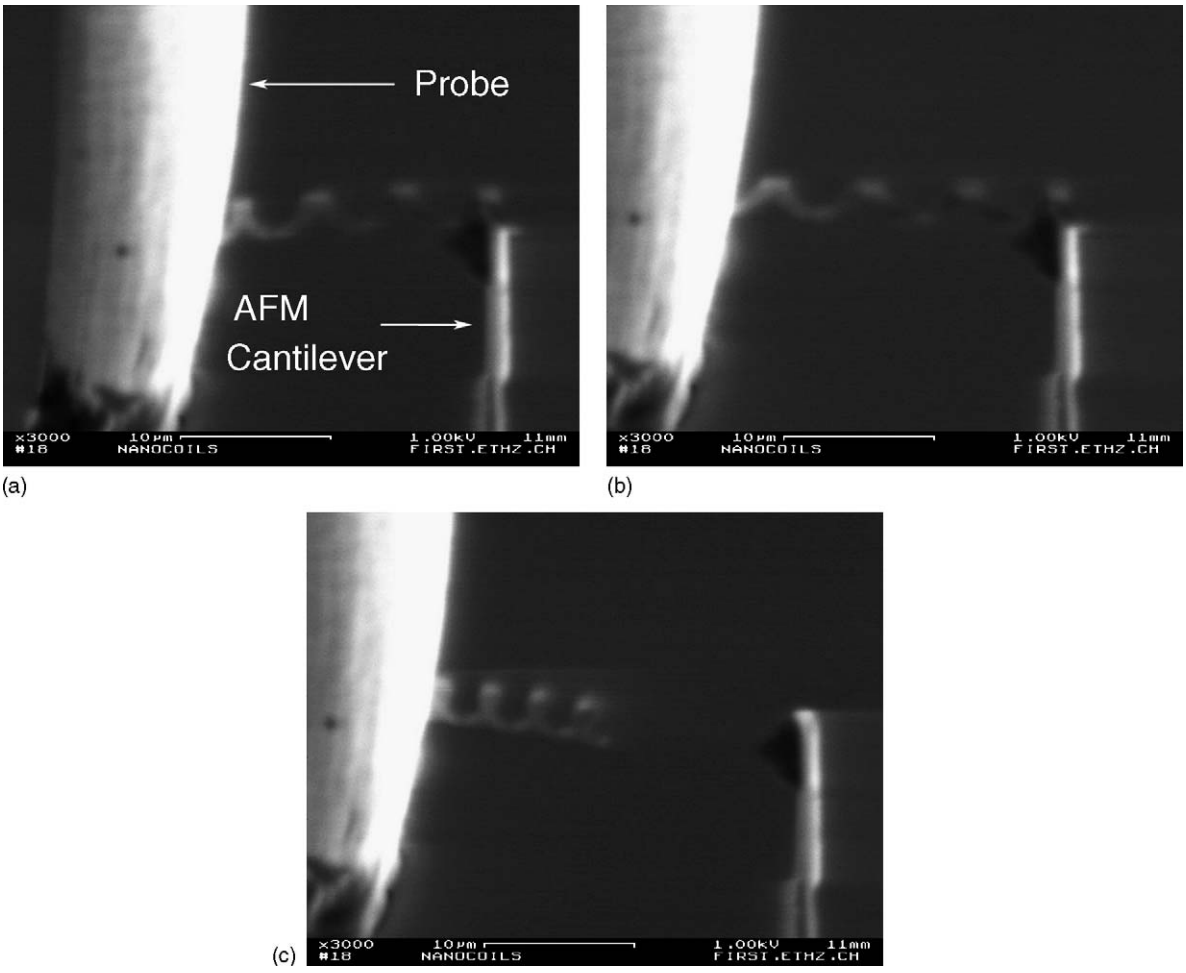

Fig. 4. SEM images of stiffness measurement with AFM cantilever.

was measured relative to the first measurement point. This was necessary because the proper attachment of the nanospring to the AFM cantilever must be checked. Afterwards, it was not possible to return to the point of zero deformation. Instead, the experimental data as presented in Fig. 6 has been shifted such that with the calculated linear elastic spring stiffness the line begins at zero force and zero deformation.

From Fig. 6, the stiffness of the spring was estimated to be 0.0233 N/m, which is approximately three times lower than the AFM cantilever stiffness. The linear elastic region of the nanospring appears to extend to a deformation of 4.5 μm. An exponential approximation was fitted to the nonlinear region. When the applied force reached 0.176 μN, the attachment between the nanospring and the AFM cantilever broke (Fig. 4c). The error bars in Fig. 6 represent the uncertainty in the deflection of the AFM cantilever and the nanospring given by the resolution of the SEM (1 μm at 3000× magnification).

In order to estimate the maximum elastic deformation of the nanosprings, a nanospring was fixed directly to the conductive tape instead of fixing it to the AFM cantilever (Fig. 7a). Thus, higher forces could be applied. After a displacement of 11.4 μm the attachment between the nanospring and the conductive tape broke (Fig. 7b and c). This corresponds to an overall strain of 33% and a force of 1.51 μN according to the exponential approximation from the previous experiment (Fig. 6). The shape in Fig. 7c is similar to the original shape, indicating that certainly a majority of the strain was recovered and that the maximum elastic strain capability of the nanosprings is at least 33%.

Finite element simulation was used to validate the experimental data. The model of the nanospring in the simulation also consisted of three different layers, similar to the actual nanospring. A plot of the displacement along the axial direction for a helical structure with similar dimensions as the one in the experiment is shown in Fig. 8. The dimensions of the nanospring used in the experiment and in the finite element model are summarized in Table 1. The exact number of turns was difficult to determine because the exact region of attachment cannot be accurately identified. However, from Fig. 3c it can be determined that the number of turns of the nanospring is 5, and from Fig. 4a and b at least 4 turns were free-standing. Therefore, simulations were conducted for 4, 4.5, and 5 turns to obtain an estimate of the possible range. The nanosprings in the simulations were fixed on one end and had an axial load of 0.106 μN applied on the other end, corresponding to the maximum force for linear deformation shown in Fig. 6. The simulation results for 5 turns are shown in Fig. 8. For the spring with 4 turns the stiffness from

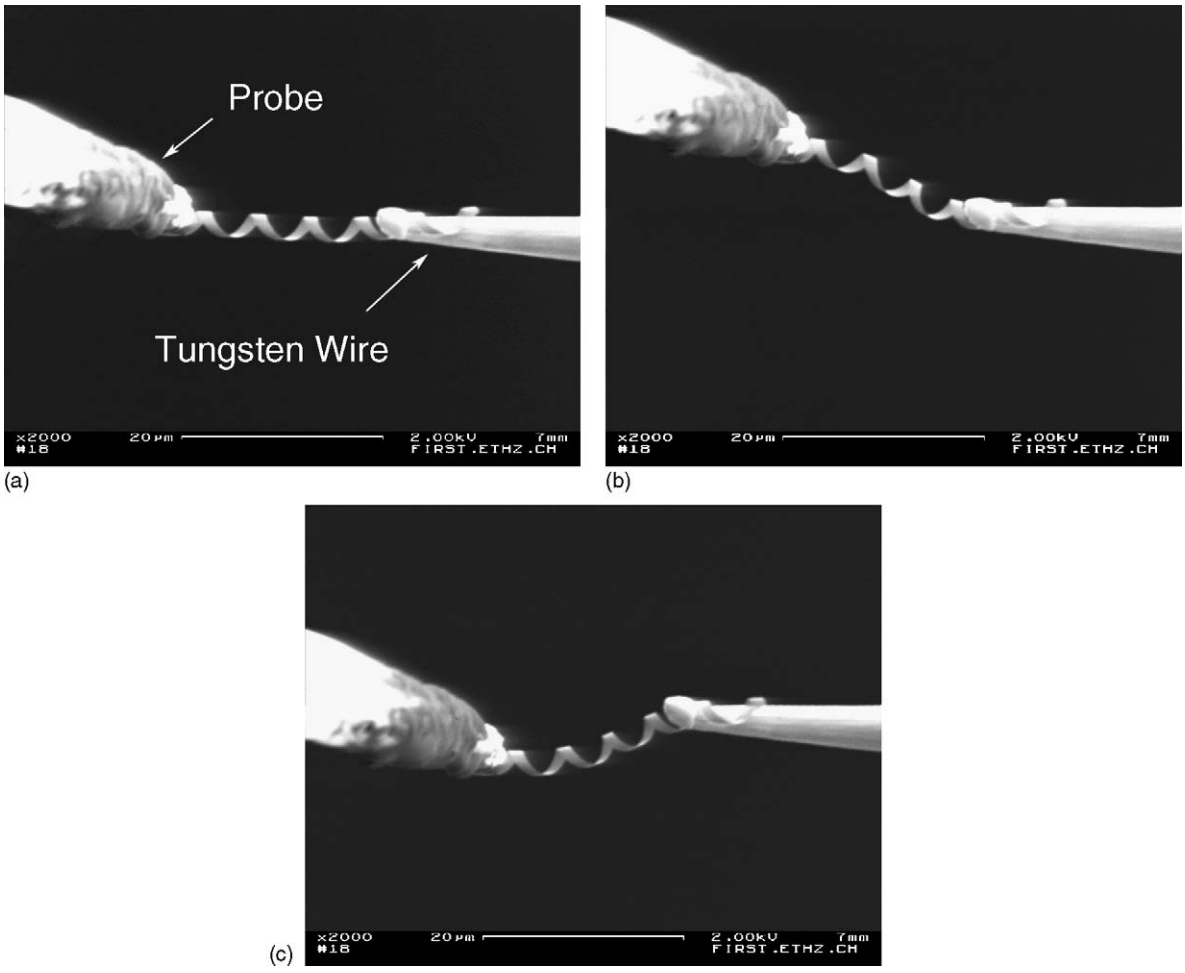

Fig. 5. Configuration of electromechanical sensors. With this configuration (a), the conductivity of the nanospring is investigated experimentally. Conductivity change caused by the deformation of nanosprings, such as in bending, (b) and (c), is a potential way to realize nano-force sensors.

simulation is 0.0302 N/m, and for the nanospring with 5 turns it is 0.0191 N/m. The measured stiffness falls into this range with 22.0% above the minimum value and 22.8% below the maximum value, and very close (+1.3%) to the stiffness of a 4.5-turn nanospring that has a stiffness of 0.0230 N/m according to the simulation. Any discrepancy between experiment and simulation may partly be caused by misalignment between the axis of the nanospring and the applied force during the experiment.

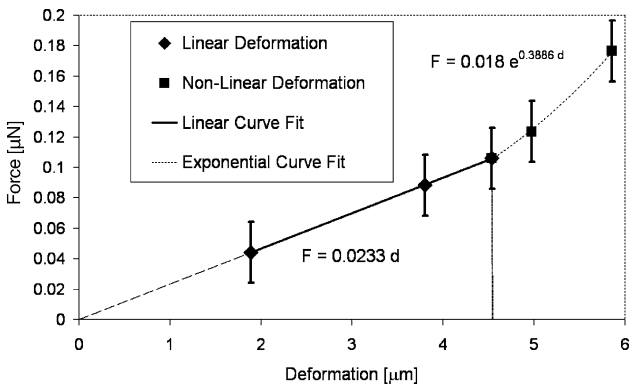

Fig. 6. Axial force vs. nanospring elongation from experiments.

Fig. 9 shows electrical characterization experiments on SiGe/Si nanosprings with 11 turns (Fig. 9a). The *I–V* curves were measured for two nanosprings. The first nanospring was characterized by sweeping the voltage from 0 to 4.5 V. For the second nanospring the range of the voltage sweep was increased to 10 V in order to capture the maximum current behavior. The *I–V* curves are illustrated in Fig. 10. They are non-linear, as expected for SiGe/Si. From Fig. 10b the maximum current was found to be 0.159 mA under a voltage bias of 8.9 V, which corresponds to a maximum current density of 5.3×10^9 A/m^2. From the fast scanning screen of the SEM, an extension of the nanospring was observed around the peak current, causing a

Table 1
Nanospring specifications used in experiments and simulations

Thickness $Si_{0.6}Ge_{0.4}$	12 nm
Thickness Si	8 nm
Thickness Cr	21 nm
Diameter	3.4 μm
Pitch	7 μm
Width of initial pattern	1.5 μm
Number of turns	4–5

The electrical characterization was done for nanosprings with no Cr layer.

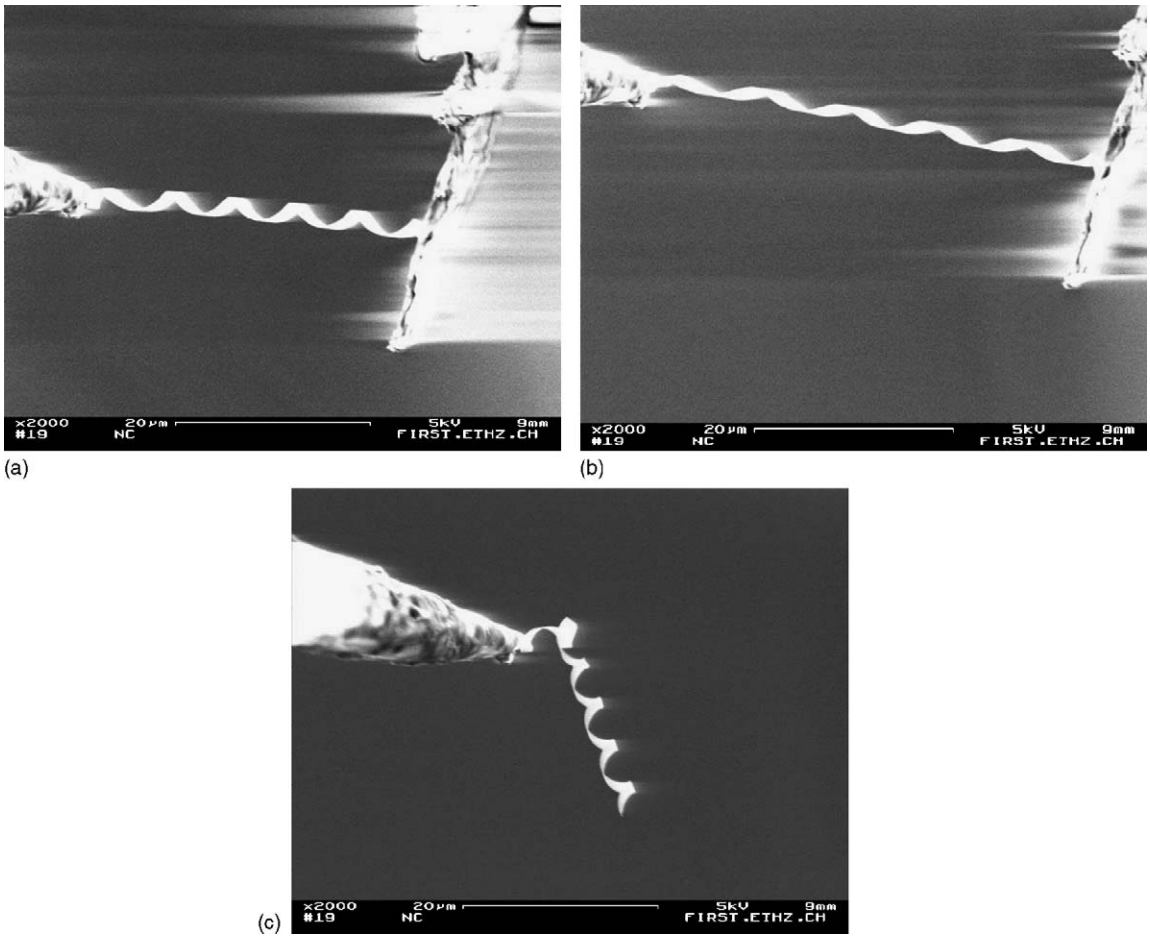

Fig. 7. SEM images of large deflection experiment. (a) Nanospring attached to conductive tape. (b) Maximum displacement ($d = 11.4$ μm, $F = 1.51$ μN) before (c) breaking of attachment.

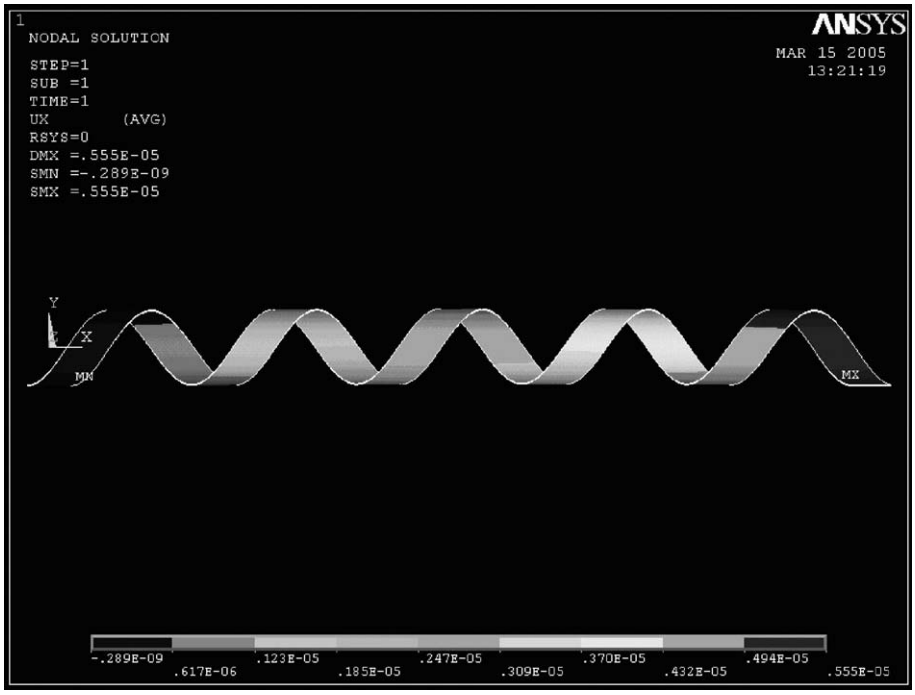

Fig. 8. Structural simulation for nanospring with five turns: axial displacement in meter for axial tensile force of 0.106 μN on one end and fixed on other end.

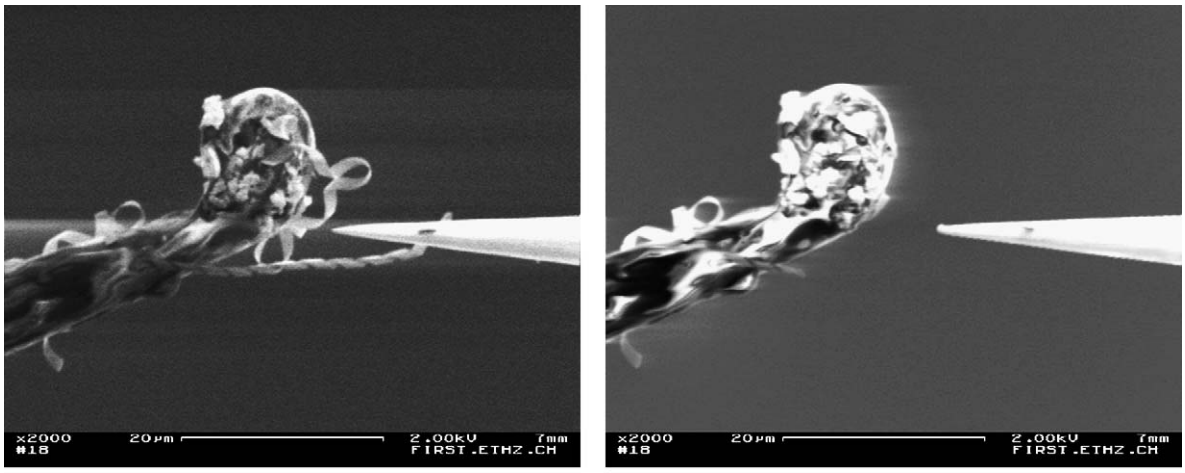

Fig. 9. (a) *I–V* curve measurement setup for SiGe/Si nanosprings. (b) During the measurement of the maximum current capability one nanospring evaporated.

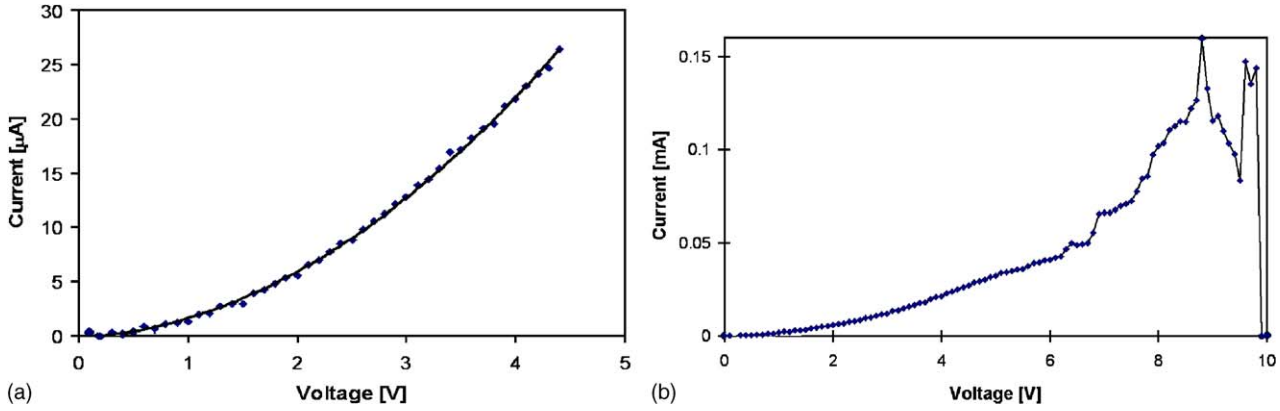

Fig. 10. *I–V* curves for two SiGe/Si nanosprings with 11 turns from (a) 0 to 4.5 V and (b) 0 to 10 V for maximum current capability measurement.

gradual drop in current. At 9.4 V, the extended nanospring is broken down (Fig. 9b), causing an abrupt drop in the *I–V* curves.

From the fabrication and characterization results, the helical nanostructures also appear to be suitable to function as inductors. They would allow further miniaturization compared to state-of-the-art micro inductors. For this purpose, higher doping of the bilayer and an additional metal layer would result in improved conductance. Conductance, inductance, and quality factor can be further enhanced if, after curling up, additional metal is electroplated onto the helical structures.

Moreover, a semiconductive helical structure, when functionalized with binding molecules, can be used for chemical sensing under the same principle as demonstrated with other types of nanostructures [17]. With bilayers in the range of a few monolayers, the resulting structures would exhibit very high surface-to-volume ratios with the whole surface exposed to an incoming analyte.

5. Conclusions

Nanospring structures were fabricated using a self-assembled fabrication process. Nanomanipulation in SEM was used for their mechanical characterization. A satisfactory agreement was obtained between the mechanical characterization of the 3D nanostructures and predictions from simulations. The tested nanospring had a low stiffness of 0.0233 N/m, and overall elastic strain of up to 14% within the linear region and up to 33% in the non-linear region, demonstrating that the nanostructures are fairly robust. Electrical characterization could also be realized through nanomanipulation. The *I–V* curves were found to be non-linear with a maximum current of 0.159 mA, which corresponds to a maximum current density of 5.3×10^9 A/m^2. The electrical performance can be further improved by integrating an additional metal layer. The nanosprings can be used as high-resolution force sensors in conjunction with visual displacement measurement. Moreover, the piezoresistive behavior of nanosprings without an additional metal layer can be used for electromechanical sensors. By varying design parameters, such as the number of turns, thickness, diameter, or pitch, a nanospring with the required stiffness can be designed through simulation. Nanomanipulation in an SEM was demonstrated as a powerful experimental technique with potential for the assembly of NEMS. The nanostructures presented in this paper are also suitable for use as inductors due to their helical

geometry and for chemical sensors due to large surface-to-volume ratios.

References

[1] S. Motojima, M. Kawaguchi, K. Nozaki, H. Iwanaga, Growth of regularly coiled carbon filaments by Ni catalyzed pyrolysis of acetylene, and their morphology and extension characteristics, Appl. Phys. Lett. 56 (1990) 321–323.

[2] X.B. Zhang, X.F. Zhang, D. Bernaerts, G.T. Vantendeloo, S. Amelinckx, J. Vanlanduyt, V. Ivanov, J.B. Nagy, P. Lambin, A.A. Lucas, The texture of catalytically grown coil-shaped carbon nanotubules, Europhys. Lett. 27 (1994) 141–146.

[3] X.Y. Kong, Z.L. Wang, Spontaneous polarization-induced nanohelixes, nanosprings, and nanorings of piezoelectric nanobelts, Nano Lett. 3 (2003) 1625–1631.

[4] X.Q. Chen, S.L. Zhang, D.A. Dikin, W.Q. Ding, R.S. Ruoff, L.J. Pan, Y. Nakayama, Mechanics of a carbon nanocoil, Nano Lett. 3 (2003) 1299–1304.

[5] K. Kaneto, M. Tsuruta, S. Motojima, Electrical properties of carbon micro coils, Synth. Met. 103 (1999) 2578–2579.

[6] S.V. Golod, V.Y. Prinz, V.I. Mashanov, A.K. Gutakovsky, Fabrication of conducting GeSi/Si micro- and nanotubes and helical microcoils, Semicond. Sci. Technol. 16 (2001) 181–185.

[7] L. Zhang, E. Deckhardt, A. Weber, C. Schönenberger, D. Grützmacher, Controllable fabrication of SiGe/Si and SiGe/Si/Cr helical nanobelts, Nanotechnology 16 (2005) 655–663.

[8] S.V. Golod, D. Grützmacher, C. David, E. Deckardt, O. Kirfel, S. Mentese, B. Ketterer, Fabrication of SiGe/Si/Cr bent cantilevers based on self-rolling of epitaxial films, Microelectron. Eng. 67 (8) (2003) 595–601.

[9] D.J. Bell, L.X. Dong, Y. Sun, L. Zhang, B.J. Nelson, D. Grützmacher, Manipulation of nanocoils for nanoelectromagnets, in: Proceedings of the Fifth IEEE Conference on Nanotechnology, Nagoya, July 11–15, 2005.

[10] G. Lin, K.S.J. Pister, K.P. Roos, Surface micromachined polysilicon heart cell force transducer, J. Microelectromech. Syst. 9 (2000) 9–17.

[11] B.L. Pruitt, W.T. Park, T.W. Kenny, Measurement system for low force and small displacement contacts, J. Microelectromech. Syst. 13 (2004) 220–229.

[12] T. Toriyama, Y. Tanimoto, S. Sugiyama, Single crystal Silicon nanowire piezoresistors for mechanical sensors, J. Microelectromech. Syst. 11 (2002) 605–611.

[13] M.A. Poggi, J.S. Boyles, L.A. Bottomley, Measuring the compression of a carbon nanospring, Nano Lett. 4 (2004) 1009–1016.

[14] T. Fukuda, F. Arai, L.X. Dong, Assembly of nanodevices with carbon nanotubes through nanorobotic manipulations, Proc. IEEE 91 (2003) 1803–1818.

[15] R. People, J.C. Bean, Calculation of critical layer thickness versus lattice mismatch for Ge_xSi_{1-x}/Si strained-layer heterostructures, Appl. Phys. Lett. 47 (1985) 322–324.

[16] U. Schnakenberg, W. Benecke, B. Lochel, NH_4OH-based etchants for silicon micromachining, Sens. Actuators A: Phys. 23 (1990) 1031–1035.

[17] Y. Cui, Q.Q. Wei, H.K. Park, C.M. Lieber, Nanowire nanosensors for highly sensitive and selective detection of biological and chemical species, Science 293 (2001) 1289–1292.

Biographies

Dominik Bell studied aerospace engineering at the University of Bristol in UK and at Purdue University in the USA and graduated from Bristol with an MEng degree after 4 years in 2002. In the same year, he started postgraduate studies at the Engineering Department of the University of Cambridge in UK. For his research in MEMS actuators and sensors and in micro mechanical testing he received an MPhil degree after 1 year. In November 2003, he joined the Institute of Robotics and Intelligent Systems (IRIS) at the Swiss Federal Institute of Technology Zurich (ETH) in Switzerland as a PhD student with a research focus on MEMS and NEMS devices and on wireless sensing and actuation.

Yu Sun is a assistant professor of the Department of Mechanical and Industrial Engineering and is jointly appointed in the Institute of Biomaterials and Biomedical Engineering and Department of Electrical and Computer Engineering at the University of Toronto. He received his BS degree in electrical engineering from the Dalian University of Technology, China, in 1996, MS degree from the Institute of Automation, Chinese Academy of Sciences, Beijing, China, in 1999, and PhD degree in mechanical engineering from the University of Minnesota, Minneapolis, in 2003. He held a research scientist position at the Swiss Federal Institute of Technology (ETH-Zurich) before joining the faculty of the University of Toronto. His research areas are MEMS design, fabrication and testing, bio-instrumentation, microrobotic biomanipulation, biomechanics, and nanofabrication and nanomanipulation.

Li Zhang received his BS degree in 2000 from Department of Materials Science and Engineering of Zhejiang University (PR China). He got his MS in 2002 from the Department of Materials Science and Engineering of Christian Albrechts University of Kiel in Germany. Since autumn of 2002, he has joined the laboratory for Micro- and Nanotechnology of Paul Scherrer Institute in Switzerland for his PhD degree. His current research work is focused on synthesis and characterization of group-IV semiconductor based microtubes and helical nanobelts.

Lixin Dong received his BS and MS degrees in mechanical engineering from Xi'an University of Technology (XUT), China in 1989 and 1992, respectively. He became a research associate in 1992, lecturer in 1995, and associate professor in 1998 at XUT. He received his PhD degree from Nagoya University in 2003, and became a assistant professor there in the same year. Currently, he is a research scientist in IRIS of ETH-Zurich. His main research interests include nanorobotic manipulation and related technologies including carbon nanotubes, nanofabrication, nano-mechanochemistry, nanoassembly, NEMS, and nanorobotics.

Bradley J. Nelson is the professor of Robotics and Intelligent Systems at the Swiss Federal Institute of Technology (ETH), Zurich and heads the Institute of Robotics and Intelligent Systems there. He received a BS (mechanical engineering) from the University of Illinois at Urbana-Champaign in 1984, an MS (mechanical engineering) from the University of Minnesota in 1987, and the PhD degree in Robotics (School of Computer Science) from Carnegie Mellon University in 1995. During these years he also worked as an engineer at Honeywell and Motorola, and served as a United States Peace Corps Volunteer in Botswana, Africa. In 1995 he became a assistant professor at the University of Illinois at Chicago, associate professor at the University of Minnesota in 1998, and professor at ETH in 2002. His most recent scientific contributions have been in the area of microrobotics, biomicrorobotics, and nanorobotics, including efforts in robotic micromanipulation, microassembly, MEMS (sensors and actuators), mechanical manipulation of biological cells and tissue, and NanoElectroMechanical Systems (NEMS).

Detlev A. Grützmacher was born in Hamburg, Germany, in 1960. He received his Diploma and the PhD degrees in physics (first class honors and Borchers medal) from the Technical University Aachen in 1988 and 1991, respectively. His undergraduate and graduate research work involved metalorganic vapor phase epitaxy in the Ga–In–As–P material system for opto-electronic applications. From 1991 to 1993 he joined the IBM Thomas J. Watson Research Center for a post doctoral position working on atmospheric pressure CVD of Si/SiGe hetero- and quantum well structures for advanced bipolar technology and resonant tunneling devices. This work was awarded by IBM with a Research Division Award. Since 1993 he is a research staff member of the Paul Scherrer Institute (PSI) in Villigen, Switzerland, working on Si based micro- and nanostructures. Currently he is heading the Si nanosystems group at PSI. He has authored and coauthored more than 150 technical papers and several patents related to these areas.